Journal of Nuclear Materials 480 (2016) 195–201

Contents lists available at ScienceDirect

Journal of Nuclear Materials

journal homepage: www.elsevier.com/locate/jnucmat

Size-dependent characteristics of ultra-fine oxygen-enriched nanoparticles in austenitic steels

Yinbin Miao [a, b, *], Kun Mo [a], Zhangjian Zhou [c], Xiang Liu [b], Kuan-Che Lan [b], Guangming Zhang [b, c], Michael K. Miller [d], Kathy A. Powers [d], James F. Stubbins [b, e]

[a] Argonne National Laboratory, Lemont, IL 60439, United States
[b] University of Illinois at Urbana-Champaign, Urbana, IL 61801, United States
[c] University of Science and Technology Beijing, Beijing 100082, China
[d] Oak Ridge National Laboratory, Oak Ridge, TN 37830, United States
[e] International Institute for Carbon-Neutral Energy Research (I2CNER), Kyushu University, Fukuoka 819-0395, Japan

HIGHLIGHTS

- The structural and chemical characteristics of nanoparticles are revealed.
- Nanoparticles' crystal structure and elemental composition are size-dependent.
- Characteristics of austenitic ODS steels are compared to that of an F/M ODS steel.
- Hypothesis about the formation mechanism of nanoparticles is proposed accordingly.

ARTICLE INFO

Article history:
Received 2 June 2016
Received in revised form
7 August 2016
Accepted 15 August 2016
Available online 18 August 2016

Keywords:
Oxide dispersion strengthened (ODS) alloy
Austenitic steels
Atom probe tomography
High-resolution transmission electron microscopy (HRTEM)
Nanostructure

ABSTRACT

Here, a coordinated investigation of the elemental composition and morphology of ultra-fine-scale nanoparticles as a function of size within a variety of austenitic oxide dispersion-strengthened (ODS) steels is reported. Atom probe tomography was utilized to evaluate the elemental composition of these nanoparticles. Meanwhile, the crystal structures and orientation relationships were determined by high-resolution transmission electron microscopy. The nanoparticles with sufficient size (>4 nm) to maintain a $Y_2Ti_{2-x}O_{7-2x}$ stoichiometry were found to have a pyrochlore structure, whereas smaller $Y_xTi_yO_z$ nanoparticles lacked a well-defined structure. The size-dependent characteristics of the nanoparticles in austenitic ODS steels differ from those in ferritic/martensitic ODS steels.

1. Introduction

Advanced structural materials with excellent mechanical performance, outstanding corrosion resistance, and exceptional radiation tolerance at elevated service temperatures are crucial for the development of advanced nuclear fission reactors and future fusion facilities [1]. Mechanical alloying of steel and yttria powders, succeeded by precisely-controlled heat treatments and thermal processing, introduces a dense distribution of ultra-fine oxygen-enriched nanoparticles into a steel matrix [2,3]. The existence of such nanoparticles alters the microstructure of conventional steels, and therefore improves the performance in multiple aspects. First, these nanoparticles are capable of enhancing mechanical strength and creep resistance by effectively pinning moving dislocations during plastic deformation and dislocation creep processes [4–6]. Additionally, the abundant interfaces created by the introduction of the nanoparticles into the matrix enhance radiation tolerance by trapping radiation-induced defects [7–10]. These two advantages are favored in solving the material challenges raised by next-generation fission reactors and fusion concepts, qualifying ODS steels as promising candidates for structural materials used in advanced nuclear applications. Previous investigations on ODS

* Corresponding author. 9700 South Cass Ave, Lemont, IL 60439, United States.
E-mail address: ymiao@anl.gov (Y. Miao).

http://dx.doi.org/10.1016/j.jnucmat.2016.08.014
0022-3115/

steels were concentrated on ferritic/martensitic (F/M) steels considering their advantages in mechanical strength and radiation swelling resistance [11–14]. However, the superiority of austenitic steels in high-temperature phase stability as well as corrosion and creep resistance can be complemented by the remarkable improvement in mechanical strength and radiation tolerance provided by oxygen-enriched nanoparticles so as to function as ideal nuclear structural materials. In addition, the radiation embrittlement caused by α'-precipitation [15] in F/M steels would not be a problem for austenitic steels. All these merits enable austentic ODS steels to be prospective materials for use in the nuclear energy industry.

As the excellent properties of ODS steels originate from the presence of ultra-fine oxygen-enriched nanoparticles, the structural and chemical characteristics of these nanoparticles control the performance of the materials. Nanoparticles in F/M ODS steels have been investigated through a series of advanced material characterization techniques. These nanoparticles are composed of Y, Ti, and O, and their composition is particle size dependent. For nanoparticles with radii exceeding ~4 nm, their phases have been confirmed to be either of the two conventional Y-Ti-O compounds, pyrochlore $Y_2Ti_2O_7$ or orthorhombic Y_2TiO_5, based on composition and structure analyses [16]. For those smaller than ~2 nm, the nanoparticles, referred to as nanoclusters (NCs) within this size range, no longer have a well-defined stoichiometry or crystal structure. The most interesting phenomenon occurs at the intermediate size regime where the experimental observations are controversial, which will be further discussed in the present study. In austenitic ODS steels, the situation seems to differ. According to the limited available literature [17–19], the nanoparticles remain crystalline until their radii drop to 2 nm, and preserve a coherent or cubic-on-cubic (CoC) orientation relationship with the austenite matrix. This difference at the atomic level between F/M and austenitic ODS steels influences the microstructural evolution of the nanoparticles and therefore, determines the performance of ODS steels. In the present study, a coordinated experimental effort was undertaken to reveal details of the differences in nanoparticle formation and to better understand the microstructural foundation for the advantages of austenitic ODS steels, towards advancing the development of austenitic ODS steels for advanced nuclear applications.

2. Experiments

2.1. Investigated materials

Three types of austenitic ODS steels were investigated for comparison with the F/M 9Cr ODS steel, as listed in Table 1. The base material powders of those four alloys were mechanically alloyed in an inert atmosphere using a planetary ball mill at 300 rpm with a ball-to-powder ratio of 5:1 for 30 h. For the austenitic steels, the powder tends to attach on the surfaces of pot and bowl. Although using pre-alloyed powder instead of mixed pure metal powders can slightly relieve this attachment phenomenon, this issue was not thoroughly eliminated in this study. Fortunately, the attachment phenomenon seems not to degrade the quality of products. Namely, the only major consequence of the attachment is reducing the powder production. Thus, the relatively low ball-to-powder ratio was adopted so as to maximize the production. As the alloying efficiency is also dependent on the impact energy of the ball milling procedure, the low ball-to-powder ratio can be compensated by appropriately adjusting the ball milling speed and endurance. The adopted combination of the ball milling speed and endurance was optimized through a series of tentative tests. The milled powder was then degassed, sealed, and consolidated through hot isostatic pressing (HIP) under a pressure of 100 MPa at 1150° for 3 h. Detailed mechanical properties enhanced by the oxygen-enriched dispersoids of the investigated materials have been examined and reported in Refs. [4,14,17,18,20].

Table 1
Nominal compositions of investigated ODS steels (wt%).

Material	Fe	Cr	Ni	C	Si	Mn	N	Mo	W	Ti	Y_2O_3
ODS 304	Bal.	18.0	8.0	–	0.15	–	–	1.0	–	0.5	0.35
ODS 310	Bal.	24.0	18.3	–	–	–	–	1.9	–	0.3	0.35
ODS 316	Bal.	16.8	13.2	–	0.7	0.4	0.2	2.5	–	0.3	0.35
9Cr ODS	Bal.	9.0	–	0.06	0.18	–	–	–	1.5	0.5	0.35

2.2. Atom probe tomography

The atom probe specimens were fabricated from 0.25 mm × 0.25 mm × 10 mm blanks that were mechanically cut from the bulk materials. The blanks were electropolished into needle-shaped specimens using the standard loop-method and electrolytes in a Simplex Electropointer [21]. In order to ensure circular cross-sections as well as an appropriate radius and taper angle, which is ideal for atom probe investigations, the needle-shaped specimens were annular milled in a Dualbeam FEI Nova 200 Nanolab focused ion beam/scanning electron microscope (FIB/SEM) system [21]. Atom probe tomography (APT) characterizations were performed in an energy-compensated CAMECA local electrode atom probe (LEAP) 4000× HR using laser-mode at a specimen temperature of 30 K, a pulse repetition rate of 200 kHz, a focus laser beam energy of either 50 or 100 pJ, and a data collection rate between 0.5% and 4.0%. The laser mode (rather than the voltage

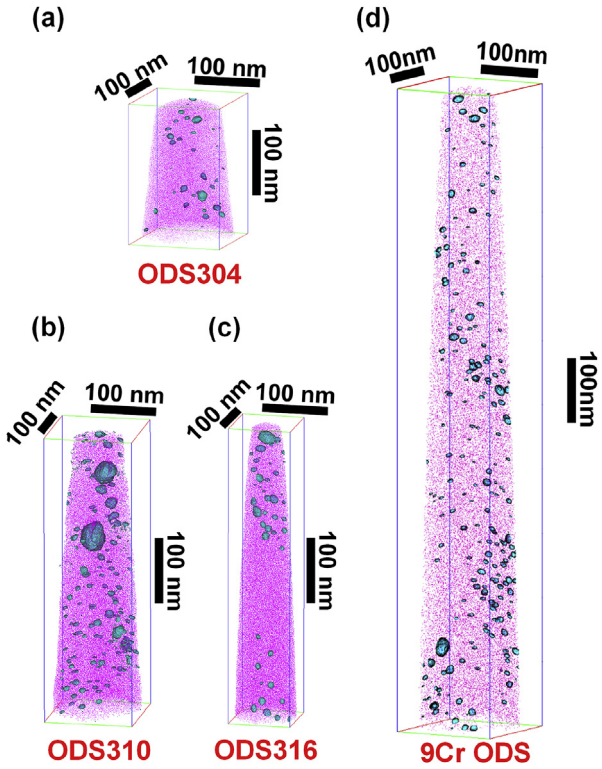

Fig. 1. The 6% O isoconcentration surfaces in investigated ODS samples: (a), (b), (c), and (d) illustrate the oxygen-enriched nanoparticle domains defined by the 6% isoconcentration surfaces in ODS 304, ODS 310, ODS 316, and 9Cr ODS, respectively. All four subfigures share the same scale bars.